ELSEVIER

Sensors and Actuators 85 (2000) 139–146

SENSORS AND ACTUATORS A PHYSICAL

www.elsevier.nl/locate/sna

Wide range semiconductor flow sensors

A. Glaninger [a], A. Jachimowicz [b], F. Kohl [a,*], R. Chabicovsky [a], G. Urban [b]

[a] *Institut für Angewandte Elektronik und Quantenelektronik and Ludwig Boltzmann Institut für Biomedizinische Mikrotechnik, Vienna University of Technology, Gusshausstrasse 27-29, A-1040 Wien, Austria*

[b] *Institut für Mikrosystemtechnik, Albert-Ludwigs-Universität Freiburg, Am Flugplatz, D-79085 Freiburg, Germany*

Received 14 September 1999; accepted 21 December 1999

Abstract

Micromachined flow sensors based on thin film germanium thermistors offer high flow sensitivities and short response times. Using the controlled overtemperature scheme, the measurable air flow velocity ranges from ± 0.01 to ± 200 m/s and the response time to large step changes of the air velocity is less than 20 ms. In the constant power mode, a signal rise time of 1.6 ms has been demonstrated by the application of shock waves. An air flow measuring range from 0.6 ml/h to at least 150 l/h has been achieved, e.g. with a rectangular flow channel of 0.54 mm^2 cross-sectional area. Using a lookup table transformation, a linearized output signal can be obtained within 25 μs.

Keywords: Flow measurement; Electrocalorimetric flow sensor; Thin film thermistor; Micromachined sensor; Constant overtemperature control

1. Introduction

There is a growing demand of micro flow sensors for industrial, automotive, domestic and medical applications. The measuring principle can be based on thermistors [1], thermopiles [2], pyroelectric elements [3], pn-junctions [4], resonating microbridges [5], Prandtl tubes [6] and several other effects. Micromachining is adopted to achieve high sensitivity, quick response and low power consumption.

One important application of flow sensors is the measuring of the air intake of combustion engines. This rate should be known for each intake stroke. Knowledge of this combustion process parameter is essential if one tries to minimize both the engines fuel consumption and the pollution of the environment. For the development of such engines, a wide velocity measuring range and high resolution monitoring of the time course of the air velocity during the stroke is desirable. Depending on the number of revolutions per minute and the geometry of the suction pipe, the air flow can change from simple pulsation to an oscillating flow with large amplitudes. The presented type of electrocalorimetric sensor is an attempt to meet the demands of such applications in terms of speed and measuring range. The thermal flow sensor is based on a heat transfer principle in which a heated body is cooled by a passing flow and the local rate of cooling depends on the flow velocity.

2. Sensor fabrication

Two thin film thermistors are placed symmetrically to a central heater on a micromachined diaphragm (Figs. 1–3). The fluid temperature, which is normally close to the substrate temperature, can be measured with two additional thermistors arranged at the rim of the silicon chip (Fig. 2). All thermistors are fabricated by evaporation of amorphous germanium onto comb-shaped electrodes. A (100) wafer has been used for the fabrication of the sensor. The size of the chip is 2×4 mm and the thickness is 0.3 mm.

A meander-type thin film resistor is used as the heater. Both platinum and nichrome have been applied as the heater material. The thin film structures were produced on a wafer, which has been covered by a silicon nitride layer. Finally, a low stress silicon nitride protective film is deposited nearly at room temperature using a PECVD process. The low deposition temperature prevents the germanium film from recrystallization. Both silicon nitride layers are forming the diaphragm of the micromachined

* Corresponding author. Tel.: +43-1-58801-35913; fax: +43-1-58801-

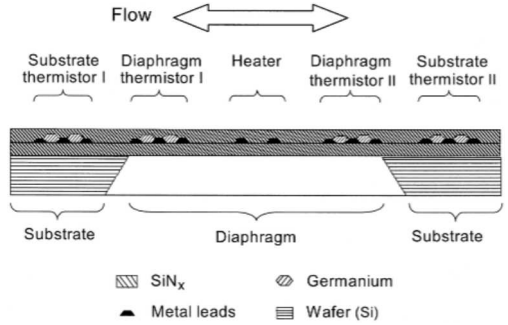

Fig. 1. Schematic cross-sectional view of the flow sensor. The total thickness of the diaphragm is 800 nm. The thermistors are shown in a symbolized form.

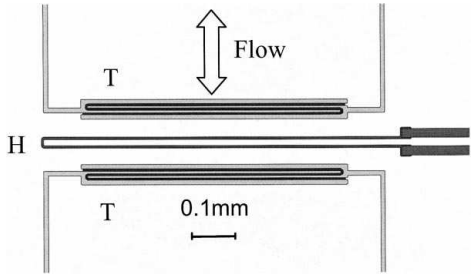

Fig. 3. Top view of the thin film structures deposited on the sensor diaphragm. The layout of the germanium thermistor *T* and the heating resistor *H* results from a compromise on fast response and high sensitivity for a flow direction as indicated.

Silicon nitride exhibits a low thermal conductivity resulting in high flow sensitivity. The thermal conductivity of silicon nitride is about 2.3 $W/m \cdot K$ as compared to 150 $W/m \cdot K$ for silicon. A further advantage of the silicon nitride diaphragm is its small thickness resulting in a small thermal conduction. However, it should be mentioned that a low thermal conductance of the diaphragm has some negative influence on the dynamic behavior of the sensor. The 800-nm-thick diaphragm used in our sensor has been proven to be very stable in a tangential flow.

Amorphous germanium exhibits high values of both the resistivity and its temperature coefficient. The temperature coefficient of resistance is approximately $-2\%/K$ and the resistivity is about 5 Ωm at room temperature. A layout as shown in Fig. 3 and a 250-nm-thick germanium film result in a resistance of 70 kΩ at 20°C. The measured resistance vs. temperature characteristic of the thermistor is shown in Fig. 4. It has been proven that the long-term stability of this characteristic is better than 0.5%/year. A noise equivalent temperature difference of 10 μK for a bandwidth of 10 Hz is achieved with this thermistor technology [7]. For comparison, Johnson noise only would limit the resolution to 4.75 μK. The observed temperature dependence of the thermistor conductance, as depicted in Fig. 5, shows that the logarithm of the conductance depends linear on $T^{-1/4}$ over a very wide temperature range. This indicates a charge transport dominated by variable range hopping [8], which is typical for many amorphous semiconductors.

The maximum electrical power rating of the heater is 40 mW if the fluid is air. However, the typical operating power is about 4 mW, which corresponds to a heater voltage of 3 V. One advantage of using high temperature-resolution thermistors is that reliable flow sensing operation requires only a small temperature difference between the heater and the fluid. The presented sensor operates with heater overtemperatures less than 25 K. However full resolution is already obtained with a heater overtemperature of 10 K. The increase of the fluid temperature caused by the heater is much smaller than the overtemperature. So the sensor is especially applicable in such cases where the heater must not cause a significant increase of the fluid temperature.

For calibration in a wind tunnel and other experimental measurements, the sensor chip is glued to a 0.15-mm-thick printed circuit board (PCB) flush fitted with the board surface (Fig. 6). For this purpose, the flexible PCB was formed using an embossing die. The dimension of this

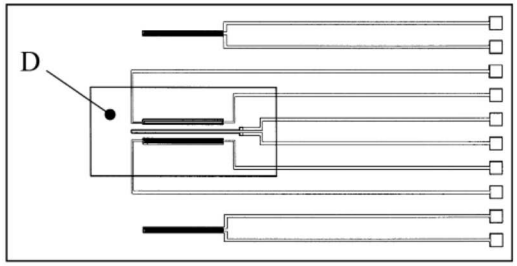

Fig. 2. Mask layout of the flow sensor chip. The chip size is 2×4 mm;

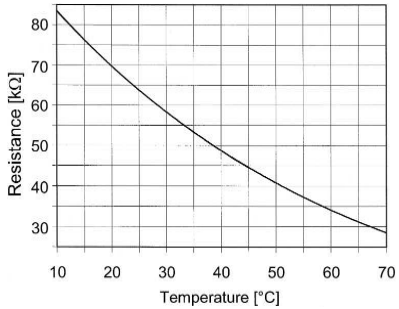

Fig. 4. Measured temperature dependence of the resistance of a thin film

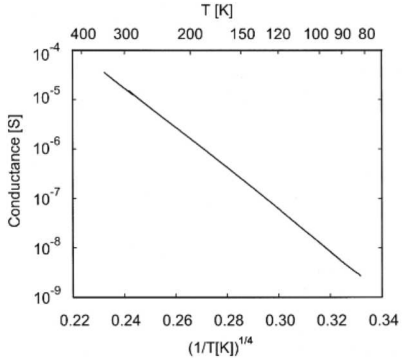

Fig. 5. Measured temperature dependence of the electrical conductance of a subtrate thermistor.

PCB in the direction of flow is 60 mm and the sensor was placed midways. The ground plane of the PCB shields the signal leads against noise coupling.

3. Electronic setup

Operating the miniaturized flow sensors with constant heating power usually result in a very limited flow measuring range. Because of efficient convective cooling, at very high flow rates, the overtemperatures of the heater and the diaphragm thermistors, as well as the sensor output signal, decrease with increasing flow. Thus, the sensor signal is not a unique function of the flow if this operating mode is used. In order to obtain a wide measuring range, a constant temperature difference between the diaphragm and the fluid is desirable and an electronic controller is needed to ensure this operating mode. However, this temperature controller has to be disabled in the case of investigations of the dynamic properties of the sensor. Then the sensor is operated in the constant power mode.

A block diagram of the used electronic setup is shown in Fig. 7. For small temperature changes, the electrical conductivity of the thermistor varies approximately linear with temperature. Thus, temperature signals were derived from each thermistor conductance. Furthermore, the conductance values of the four thermistors are transformed into voltage signals by a signal conditioning unit. An electronic PI-controller is used to establish a constant

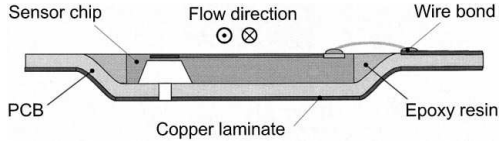

Fig. 6. Schematic cross-sectional view of the sensor mounted on the

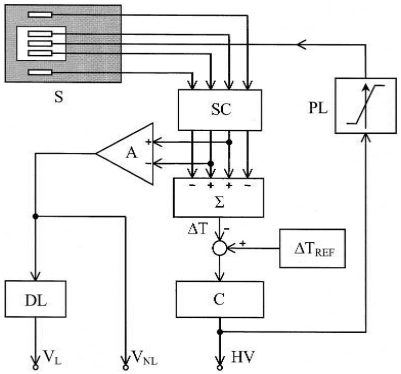

Fig. 7. Block diagram of the electronic circuit: S sensor chip, SC signal conditioning unit, Σ summing amplifier, A differential amplifier, ΔT_{REF} overtemperature setpoint, C PI-controller, PL power limiter, DL digital linearization unit, V_L linearized velocity output signal, V_{NL} nonlinear velocity output signal, HV heater voltage signal.

difference between the temperature mean of the two diaphragm thermistors and the temperature mean of the two substrate thermistors [9]. This corresponds closely to a constant overtemperature condition of the heater with respect to the fluid temperature over the whole flow range. As the heater voltage, rather than the heater power, is controlled by the electronic controller, care has to be taken for the right polarity of the output signal.

The dynamic behavior of the controlled system, which is determined by the thermal properties of the sensor diaphragm, restricts the dynamic behavior of the presented temperature tracking controller. These thermal properties can be characterized by a temperature transportation time and a thermal delay time, both of them can easily be estimated by observing the diaphragm thermistor response caused by voltage steps applied to the heater. The transportation time t_P needed for the transfer of heat from the heater to the thermistors is nearly independent of the fluid flow. It is given to a first approximation by [10]:

$$t_P = d^2/2\alpha, \quad (1)$$

where d is the distance between the heater and a diaphragm thermistor (75 μm), and α denotes the thermal diffusivity of the diaphragm material SiN_x (1.6 mm^2/s [11]). The measured value of 1 ms is in good agreement with the calculated value of 1.76 ms. Furthermore, a thermal delay time t_D was observed, which arises as a consequence of the thermal mass of the diaphragm and the resistance to heat transport processes. It amounts to 9 ms at zero flow and decreases slightly with increasing fluid flow.

The temperature difference between the two diaphragm thermistors, used for the generation of the output signal, is a nonlinear measure for the flow velocity of the medium (Fig. 8). An output signal proportional to the flow velocity

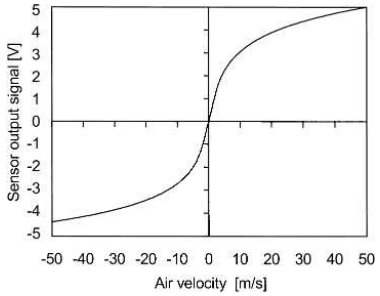

Fig. 8. Output signal prior to the linearization of the sensor signal as a function of the air velocity (calibration curve). The asymmetry of the curve is caused by a mask-misalignment during sensor fabrication.

signal and performing a special lookup table transformation followed by a digital to analog conversion. It can be used, for example, to compensate for an asymmetry of the sensor structure and to calibrate the sensor for different flow geometry. The chosen resolution for digitizing the sensor signal was 12 bits. Performing the lookup table transformation, the digital raw value is interpreted as the 12-bit address pointing to the read-only memory location, which contains the digital equivalent of the linearized value. Therefore, a unique sensor characteristic is a necessary precondition for the applicability of this linearization method. The digital value can be transferred to a computer or converted to an analog signal, which is now proportional to the actual flow. A great advantage of this linearization is that any digitized information about further interfering physical parameters, like the ambient temperature or humidity, can be put into lookup tables with an address space of more than 12-bit width. These wider tables have to contain a set of sensor characteristics according to ambient temperature or humidity variations.

4. Experiments and results

4.1. Sensor properties at stationary flow

To obtain the free field calibration curve shown in Fig. 8, the PCB carrying the sensor was placed along the direction of flow in a wind tunnel. The PCB design ensures a defined boundary layer over the whole stationary flow range.

To estimate the achievable measuring range for flow rates, a sensor was mounted flush with the wall of a 10-mm-long rectangular flow channel of 1.2-mm width. The height of this flow channel could be chosen in steps of 0.15 mm using the appropriate number of metal spacers.

Low flow rates of air were established by syringe pumps whereas a standard mass flow controller was used in the high flow rate regime. Fig. 9 demonstrates the

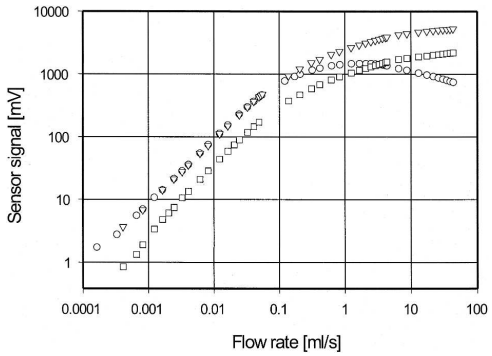

Fig. 9. Measured sensor signal vs. flow rate characteritics for a flow channel of 0.54 mm^2 cross-sectional area. Two values for the overtemperature were used: 23 K (▽) and 10 K (□). A constant power characteristic (○) is shown for comparison.

which spans more than five orders of magnitude. The sensor signal is derived from the temperature difference without linearization. For a rectangular flow channel of 0.45-mm height and 1.2-mm width, a measuring range from 0.6 to at least 150 000 cm^3/h was observed. This range corresponds to average flow velocities ranging from 0.31 mm/s up to 75 m/s. In Fig. 9, the two monotonous increasing characteristics belong to the constant overtemperature mode using 23 and 10 K overtemperature. The third characteristic, which corresponds to an operation at a constant power of 4 mW, shows a decreasing sensor signal at high flow rates. The use of the constant overtemperature scheme extends the flow rate measuring range by more than two orders of magnitude compared to the constant power scheme.

The corresponding dependence of the heater power on the flow rate, as shown in Fig. 10, suggests that this quantity could be used as a linear measure of the mass flow rate if the pressure is sufficiently constant. This mass flow regime can be understood from the heat transport

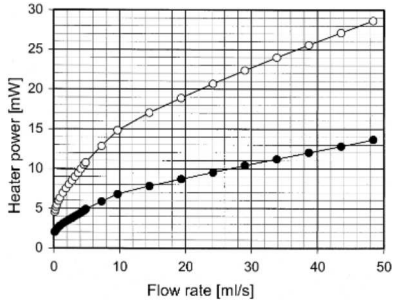

Fig. 10. Heater power as a function of flow rate for a flow channel of 0.45×1.2 mm cross-sectional area. Two values for the overtemperature

equation and the conditions in the flow channel by the following reasoning.

For an ideal incompressible fluid, the thermal energy transport equation can be written as [12]:

$$\rho c_p \left(\frac{\partial T}{\partial t} + \vec{v} \cdot \nabla T \right) = \lambda \nabla^2 T, \quad (2)$$

where ρ denotes the mass density, c_p the specific heat and λ the thermal conductivity of the fluid. $\vec{v}$ represents the velocity of the volume element of consideration, t the time variable, T the temperature and ∇ the nabla operator.

If we use a cartesian coordinate system and take x for the direction of flow, y for the direction normal to the surface and the flow and if we further neglect any temperature variation in the z-direction and if we limit our considerations to the stationary flow then Eq. (2) reduces to:

$$\rho c_p v_x(y) \frac{\partial T}{\partial x} = \lambda \left(\frac{\partial^2 T}{\partial x^2} + \frac{\partial^2 T}{\partial y^2} \right), \quad (3)$$

where $v_x(y)$ denotes the velocity parallel to the x-direction. The average of $v_x(y)$ multiplied by the flow channel cross-section gives the actual flow rate. Because of the constant overtemperature mode, the average temperature of the diaphragm is kept constant. Fig. 9 tells one that at the highest flow rates, the shape of the temperature profile along the sensor diaphragm, the x-direction, does not change appreciable with the flow rate. Thus, the derivative of T with respect to x and the first term on the right-hand side of Eq. (3) are fairly constant for this flow regime. By energy conservation principles, a change of the flow velocity $v_x(y)$ must then provoke a corresponding change of the second term of the right-hand side of Eq. (3).

At high flow rates, the power dissipated by the heater does not penetrate deeply in the flowing fluid and a part of the fluid passing the diaphragm keep its initial temperature. This corresponds to:

$$\frac{\partial^2 T}{\partial y^2} = 0 \text{ and } \frac{\partial T}{\partial y} = 0 \quad (4)$$

for sufficiently large values of y inside the flow channel. It can then be shown by integration of Eq. (3) with respect to variable y that if the shape of the flow velocity profile $v_x(y)$ does not change appreciable with the flow rate, not only $\partial^2 T/\partial y^2$, but also $\partial T/\partial y$, varies linear with the flow rate. The latter quantity, taken at the diaphragm surface, is directly related to the power dissipated by the heater. Thus, in the high flow regime, a linear dependence of the measured heater power on the flow rate can be expected for the constant overtemperature mode. A close inspection of Fig. 10 shows at least two regions of nearly linear flow dependence of the sensor signal which may be attributed to

4.2. Dynamic properties of the sensor

For the studies of further sensor properties, the PCB was placed at the center of a 1-m-long acrylic glass tube of 50-mm diameter. A continuous flow was supplied by the suction of a speed controlled exhauster. The dynamic properties of the sensors were tested with step changes of the air velocity, acoustic air oscillations and shock waves. Step changes of the air velocity were produced by abrupt blocking the inlet of the tube or by shock waves that were generated by blasting balloons in a 0.25-m-long vessel mounted at one end of the tube.

Due to the sensor layout (Figs. 2, 3) and the small thickness of the diaphragm, these sensors respond very quickly to step changes of the air velocity. In the constant overtemperature mode, the sensors show a response time of less than 20 ms to large step changes of the air velocity, depending on both the size and the direction of the step. Fig. 11 shows the sensor response to an abruptly stopped flow and the controlled overtemperature mode.

A Bode plot of the sensor signal for small acoustic flows is depicted in Fig. 12. The sensor was operated in the constant power mode. Acoustic flows at various frequencies were generated by a sinusoidal driven loudspeaker and the sound pressure level was kept constant using the response of a reference microphone. This figure is of qualitative nature only because no calibrated sound equipment was available. The data correspond to a double pole at a frequency of 1 kHz, which is in reasonable agreement with the rise time data. The slope of -40 dB/decade of the diagram can be attributed to two mechanisms. Firstly, there is a delay by the thermal mass and the thermal conductivity of the diaphragm and, secondly, there is a decrease of convective heat transport with increasing frequency. For constant sinusoidal acoustic flow, the amplitude of the air movement is inverse proportional to the frequency of the oscillation [13] and, thus, the convective heat transport decreases with increasing frequency.

Further demonstrations of the excellent dynamic properties of the sensor are given in Figs. 13–15.

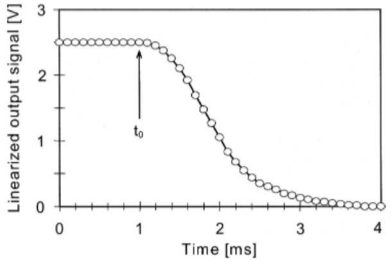

Fig. 11. Response to a flow step from 25 m/s to 0 at t_0 for the constant

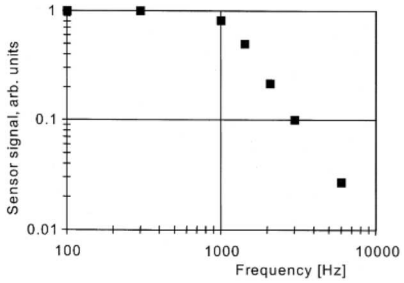

Fig. 12. Bode-plot of the acoustic flow signal of the sensor for the constant power mode.

The signals shown in Fig. 13 were recorded using the constant overtemperature mode with the PCB carrying the sensor located in the 50-mm acrylic glass tube. The lower trace shows the response of the sensor to a shock wave generated by a bursting balloon. The shock wave efficiently stimulates acoustic oscillations corresponding to resonances of the one-sided closed volume consisting of the tube and the balloon vessel having a total length of 1.25 m.

The oscillation frequency that is predominant in the sensor signal of Fig. 13 corresponds to a wavelength close to 1 m, which is approximately 4/5 of the total length. At this resonant frequency, the acoustic flow is enhanced according to the position of the sensor, which was placed at 0.5 m or half a wavelength from the open end of the tube. At this position, the acoustic flow of the standing sound wave has a maximum. In the upper part of Fig. 13, the course of the controller output voltage is plotted. As can be seen, the convective heat transfer is related to the oscillation amplitude of the sensor signal. But the heater voltage trace does not follow the acoustic oscillations indicating that the temperature average of both diaphragm thermistors oscillates much less than their temperature difference.

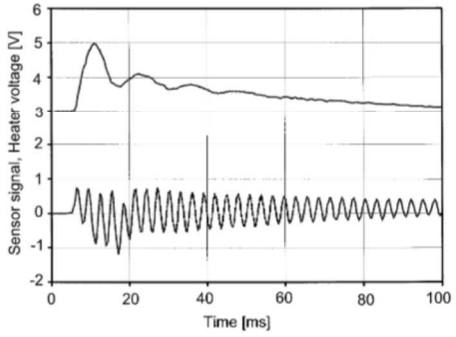

Fig. 13. Sensor and heater voltage signal in response to a shock wave in a cylindrical tube. The oscillation frequency of 340 Hz corresponds to a wavelength of nearly 1 m whereas the length of the one-sided closed tube

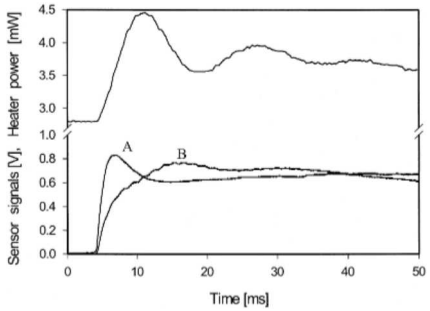

Fig. 14. Sensor responses and power controller response to large flow steps. Trace A: constant power mode, no orifice. Trace B: constant overtemperature mode, flow limited by an orifice of 2-mm diameter to about 2% of the value of trace A. Upper trace: heater power corresponding to the signal of trace B.

It can be concluded from the sensor signal shown in Fig. 13 that mainly acoustic resonance oscillations were exited by the shock wave due to the flow channel dimensions of this arrangement. To estimate the rise time of the sensor in response to a step of the flow, a tube of smaller diameter and increased length seems desirable.

Therefore, in conjunction with shock waves, a further arrangement was used consisting of a flow channel of 15-mm diameter and a flow sensor mounted flush to the surface of a 0.5-mm-thick PCB board of 15-mm width. The PCB surface was placed in a symmetry plane of the flow channel. This flow channel was then attached to the balloon vessel. A PVC hose of 3/4-in. diameter and 8.5-m length was used as an elongation of the flow channel in order to get a propagation delay of about 25 ms, which is sufficient to avoid the appearance of reflected waves generated at the end of this long flow channel in all presented signal recordings. Two sensor positions, namely 300 mm from the flow channel entrance and at the end of the hose, were investigated.

In Fig. 14, sensor responses to shock waves are shown. The sensor was placed at the end of the hose and two operating modes were compared. In the first case, the sensor was operated in the constant power mode and no

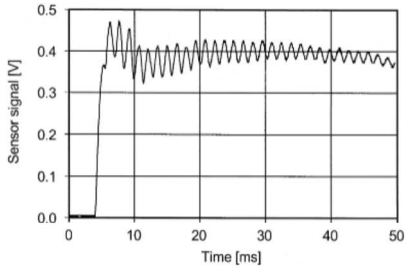

Fig. 15. Sensor response to a step change of flow generated by a shock

flow limiting orifice was used (trace A). A large overshoot occurs, which is a consequence of the thermal mass of the sensor diaphragm in conjunction with the strong nonlinearity of the sensor's stationary flow characteristic, if it is operated in the constant power mode as can be seen in Fig. 9. After a few milliseconds, the diaphragm is cooled down by the flow and, consequently, the sensor signal decreases in spite of the high flow rate. Comparing the signal level with the constant power trace of Fig. 9, one can roughly estimate that under the given conditions the air flow velocity is of the order of 100 m/s. For trace B, the sensor was operated in the constant overtemperature mode and the flow was limited by an optional orifice of 2-mm diameter, which was placed at the entrance of the flow channel. To a first approximation, the reduction factor for the acoustic flow is given by the ratio of the cross-sectional areas of the orifice and the flow channel. Thus, the flow reduction factor is 55 compared to trace A. The rise time of trace B is about 8 ms and the corresponding time course of the heater power is shown in the upper part of Fig. 14. The temperature controller reacts within milliseconds and, as a consequence, there is no immediate overshoot of the signal B. A delayed small undulation visible in that trace may be caused by the transient behavior of the heater power.

Fig. 15 shows the response to a shock wave of reduced step height and a sensor position 300 mm from the orifice of 1-mm diameter. This small orifice reduces the acoustic flow to such levels where a nearly linear sensor response could be assumed even for the constant power mode. A rise time (10% to 90% of the sensor signal) of 1.6 ms was obtained for this case indicating that the rise time of the flow step itself is shorter than this value. The signal step corresponds to a flow step from nearly zero to about 0.55 m/s. On the top of the step, oscillations with a frequency of 680 Hz corresponding to a wavelength of 500 mm are visible. These oscillations can be attributed to an acoustic resonance inside the balloon vessel having a length of 250 mm. Subtraction of these oscillations reveals that there is a small overshoot of the sensor signal, which is once again a consequence of the thermal mass of the diaphragm and the higher diaphragm temperatures prior to the flow step.

A rough estimate of the burst pressure of the balloon is possible from the recorded signal. Acoustic flow v and sound pressure p are related by [13]:

$$p = v\rho c, \tag{5}$$

where ρ denotes the mass density and c the velocity of sound for the fluid. For air at ambient temperature, the density is 1.21 kg/m^3 and c equals 344 m/s [13]. For a flow of 0.55 m/s, Eq. (5) leads to a sound pressure of 229 Pa. This results in a burst pressure of 51.5 kPa, since the burst pressure is reduced by the ratio of the orifice area to the channel cross-section, which is 225 in our case. Measured burst pressures range from 0.25 to 1 bar, depending

Placing the sensor at the end of the 8.5 m flow channel, a rise time of 2.2 ms was observed under equal conditions. The slight increase of the transient time indicates that for these channel dimensions a slight frequency dependence of the attenuation of sound waves occurs, but its contribution to the rise times shown in Fig. 14 is nearly negligible. This is in good agreement with the expectation. The theoretical value of the extinction coefficient μ for the wave propagation in a tube is given by [14]:

$$\mu = \frac{U}{2\sqrt{2}\,cA}\sqrt{\nu\omega}\,, \tag{6}$$

which depends on both the flow channel circumference U and its cross-sectional area A, the cinematic viscosity ν of the fluid and the angular frequency ω. With the viscosity of air $\nu = 1.51 \times 10^{-5}$ m^2/s, a flow channel of 15-mm diameter and an angular frequency of, e.g. $\omega = 10^4$ s^{-1} a value of $\mu = 0.0376$ m^{-1} results. With this value, a sound wave attenuation ratio of 0.73 or -2.8 dB is obtained for a flow channel of $L = 8.5$-m length using the well-known exponential dependence from μ and L. This weak damping, as well as the slight dependence of μ on the square root of ω, is in good agreement with the fast transient of the shock wave observed at the end of the flow channel.

5. Conclusions

The extraordinary high temperature resolution of typically better than 10^{-4} K offered by amorphous germanium [1] as well as the excellent matching of thermistor resistances result in a high flow sensitivity. Miniaturized flow sensors based on germanium thermistors are fast responding and can span at least four orders of magnitude of the flow velocity if they are operated in the constant overtemperature mode. Due to the high temperature sensitivity of the thermistors, an overtemperature of only a few Kelvin is sufficient for an extreme wide measuring range.

We have developed a sensor, which is capable of measuring air velocities ranging from 0.01 to about 200 m/s in a flow tube of 50-mm diameter. The results suggest that the same measuring range can be achieved for free flows of air.

With proper flow channel arrangements, a measurable range of flow rates spanning more than five orders of magnitude can be achieved. Further extension of the upper limit of this flow range is feasible if the linear dependence of the dissipated power on the flow rate is used and a slower response is acceptable.

A simple method for the generation of fast transients of the flow velocity was established, which yields flow steps in the millisecond regime. Shock waves can be used in conjunction with proper flow channels as a convenient way to study the transient behavior of miniaturized flow sensors. The rise time of the sensor signal in response to

Our experiments show that the sensor is also applicable to acoustic flow measurements. We have detected sound frequencies up to 13 kHz. In response to acoustic flows, a −40 dB/decade slope was observed with a corner frequency of 1 kHz. The properties of this acoustic flow sensor are comparable to the so called μ-flown [15].

Besides its high speed, the newly developed linearization method offers a flexible way to calibrate the sensor output signal for the quantity to be measured or for a specific flow channel geometry. By this way, it is also possible to compensate for a small asymmetry of a sensor and fluid temperature variations.

The wide measuring range of the sensor calls for a linearization circuitry having a resolution of 14-bit plus sign. Alternative control circuits may be necessary for special applications [16]. Solutions based on digital controllers will be considered in our future work. Furthermore, we try to achieve shorter response times by an advanced sensor design.

Acknowledgements

We gratefully acknowledge financial support by the Forschungsförderungsfonds für die gewerbliche Wirtschaft (Austria) and by the company AVL (Austria).

References

[1] H. Kuttner, G. Urban, A. Jachimowicz, F. Kohl, F. Olcaytug, P. Goiser, Microminiaturized thermistor arrays for temperature gradient, flow and perfusion measurements, Sens. Actuators, A 25–27 (1991) 641–645.
[2] D. Moser, R. Lenggenhager, H. Baltes, Silicon gas flow sensors using industrial CMOS and bipolar IC technology, Sens. Actuators, A 25–27 (1991) 577–581.
[3] H.Y. Hsieh, A. Spetz, J.N. Zemel, Pyroelectric anemometry: vector and swirl measurements, Sens. Actuators, A 49 (1995) 141–147.
[4] R. Kersjes, F. Liebscher, E. Spiegel, Y. Manoli, W. Mokwa, An invasive catheter flow sensor with on-chip CMOS readout electronics for the on-line determination of blood flow, Sens. Actuators, A 54 (1996) 563–567.
[5] S. Bouwstra, R. Legtenberg, H.A.C. Tilmans, M. Elwenspoek, Resonating microbridge mass flow sensor, Sens. Actuators, A 21–23 (1990) 332–335.
[6] O. Berberig, K. Nottmeyer, J. Mizuno, Y. Kanai, T. Kobayashi, The Prandtl micro flow sensor (PMFS): a novel silicon diaphragm capacitive sensor for flow-velocity measurement, Sens. Actuators, A 66 (1998) 93–98.
[7] G. Urban, A. Jachimowicz, H. Ernst, S. Seifert, J. Freund, Ultrasensitive flow sensors for liquids using thermal microsystems, CDROM Proc. Eurosensors XIII, Den Haag, Sept. 12–15, 1999.
[8] N.F. Mott, E.A. Davies, Electronic Processes in Noncrystalline Materials, Clarendon Press, Oxford, 1979.
[9] A. Glaninger, Electrocalorimetric air flow measurement with a micromachined semiconductor sensor, Diploma thesis, Vienna University of Technology, 1998.
[10] P. Frank, R. von Mises (Eds.), Differentialgleichungen der Physik Band 2 Vieweg, 1961, p. 541.
of low-residual stress, silicon rich, LPCVD silicon nitride films, Sens. Actuators, A 23 (1996) 856–860.
[12] H. Gröber, S. Erk, U. Grigull, Die Grundgesetze der Wärmeübertragung, Springer, 1981, pp. 205–209.
[13] M. Heckl, H.A. Müller (Eds.), Taschenbuch der Technischen Akustik Springer, 1975, p. 7.
[14] L. Cremer, H.A. Müller, Die wissenschaftlichen Grundlagen der Raumakustik Band 2 Hirzel, 1976, pp. 69–72.
[15] H.E. de Bree, P. Leussink, T. Korthorst, H. Jansen, T.S.J. Lammerink, M. Elwenspoek, The μ-flown: a novel device for measuring acoustic flows, Sens. Actuators, A 54 (1996) 552–557.
[16] J. Steurer, F. Kohl, Adaptive controlled thermal sensor for measuring gas flow, Sens. Actuators, A 65 (1998) 116–122.

Biographies

Rupert Chabicovsky was born in Melk, Austria in 1940. He received his Dipl.-Ing. degree and his PhD degree in Electrical Engineering from the Technical University Vienna in 1965 and 1968, respectively. He has been with the Institute of Applied Electronics and Quantum Electronics and former Institutes since 1966 and he has been a professor in the Faculty of Electrical Engineering at the Vienna University of Technology since 1979. His research areas include microelectronic technologies, thin-film sensors and optical sensor systems.

Franz Kohl was born in Vienna, Austria in 1947. He joined the Institut für Physikalische Elektronik at the Technical University Vienna in 1972 and worked on photoconductive detectors for the far infrared. He received his Dr. tech. degree in Electronic Engineering in 1978. His research interests include miniaturized sensors produced by thin film technology. He has been responsible for the characterization of miniaturized thermal sensors since he joined the Institute of Applied Electronics and Quantum Electronics in 1981.

Alexander P. Glaninger was born in Vienna, Austria in 1969. He received his Dipl.-Ing. degree in Electrical Engineering from the Vienna University of Technology in 1999. His diploma thesis concerns electrocalorimetric air flow measurements with a micromachined semiconductor sensor. He is currently with VATECH ELIN in Vienna.

Gerald A. Urban received BS and MS degrees in Physics and a PhD of Technical Sciences in Sensor Technology from the Technical University of Vienna, Austria, Inauguration in 1994. From 1979 to 1981, he was employed at the Department of Neurosurgery, University Hospital Vienna. In 1982, he became an Assistant Professor in the Department of Electrical and Electronics Engineering. In 1985, he co-founded a venture capital company (OSC) in USA and Austria. Since 1995, he has been the leader of the Ludwig Boltzmann Institute for Biomedical Microengineering in Vienna. His research activity includes the research and development of sensor applications on human beings and microthermistors. Recently, nanosystem and microsystem technology is the main field of interest developing chemosensors and biosensors implemented in microsystems. He has published 92 refereed papers, 12 book chapters and holds 10 patents. Since 1997, he is a full Professor of Sensors and Vice Dean of the Faculty of Applied Science at the Albert Ludwig University Freiburg, Germany.

Arthur Jachimowicz was born in Nisko, Poland in 1947. He graduated in Engineering, Solid-State Electronics from the Technical University Warsaw in 1971 and worked afterwards in the semiconductor industry in Warsaw. From 1977 to 1997, he was an Assistant in the Department of Electrical Engineering at the Technical University in Vienna, Austria. He received his Dr. tech. degree in Electronic Engineering in 1997. He works currently in the Sensor Department of the University Freiburg, Germany. His research interests include developing and optimising of thin film processes for manufacturing of miniaturised electrochemical and thermal